A SIMPLE MODEL TO ACCOUNT FOR THERMAL CAPACITY IN BOREHOLES

V. Godefroy, Graduate student, Département de Génie Mécanique, Polytechnique Montréal, Montréal, Québec, Canada
M. Bernier, Professor, Département de Génie Mécanique, Polytechnique Montréal, Montréal, Québec, Canada

Abstract: A relatively simple borehole heat exchanger model that accounts for grout and fluid thermal capacity has been developed and is presented in this paper. The quasi 3D model divides the borehole into successive layers. The cross-sections of each layer are modeled by the so-called 'thermal resistance and capacity models' (TRCM) approach. The resulting TRCM model has been implemented as a component (TYPE) in the TRNSYS environment. This enables its use with other models (building, heat pumps, etc.) in annual energy simulations.

The model has been compared successfully against other models. Results of annual simulations of a typical ground source heat pump system show that neglecting fluid and grout thermal capacities leads to a ≈ 3% over prediction of the heat pump energy consumption. The overestimation increases when boreholes are undersized or when the heat pump COP variation with the entering water temperature is high.

Key Words: borehole, heat pump, thermal capacity, TRCM, simulation

1 INTRODUCTION

Most ground heat exchanger models assume a steady-state condition, thereby neglecting the thermal capacity associated with the fluid and the grout. This is a good assumption when the borehole operates almost continually approaching a quasi-steady-state condition. However, it becomes questionable when boreholes operate intermittently. One example of such a behavior is when a ground source heat pump system is switched on-and-off to meet the building load.

Kummert and Bernier (2008) simulated a residential ground source heat pump system with steady-state and transient models using, respectively, the DST model (Hellström, 1991) and the EWS model (Wetter & Huber, 1997) for the borehole heat exchanger. They concluded that steady-state models can overestimate the heat pump energy consumption by as much as 75% in extreme cases.

Salim-Shirazi and Bernier (2013) also studied the effects of borehole thermal capacity by using a one-dimensional transient ground heat exchanger model based on an equivalent geometry in which a U-tube is modeled by an equivalent single pipe. They performed annual simulations with and without borehole thermal capacity. They estimated that the annual COP predicted is approximately 4.5% higher when borehole thermal capacity is included.

The present paper follows up on these previous studies. It focuses on the effects of fluid and grout thermal capacities on the heat pump energy consumption. A new borehole model based on the thermal resistance and capacity concept (often referred to as TRCM) is developed. The proposed model is first compared to other models and then used in annual simulations of a typical ground source heat pump system.

2 PROPOSED TRCM MODEL

The proposed model is based on the works of Pasquier and Marcotte (2012), Bauer et al. (2011), and Zarella et al. (2011). The quasi 3D model divides the borehole heat exchanger into n_L layers along the borehole axis. The cross-sections of each layer are modeled using the so-called 'thermal resistance and capacity models' (TRCM) approach. The modeled TRCM network is presented in Fig. 1c. For a single U-tube borehole the circuit has 8 nodes in each layer. The model can also be adapted for a double U-tube borehole but is not presented here.

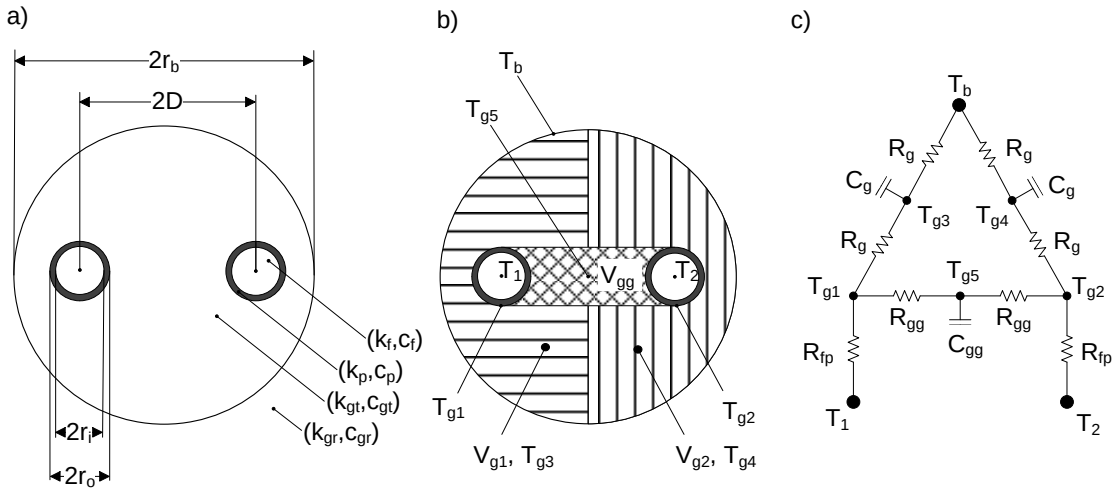


Figure 1: Modeling of the borehole: a) Horizontal cross-section of a single U-tube borehole, b) Various zones in the grout region, and c) proposed TRCM circuit

The circuit integrates the grout thermal capacity in three separate regions. The two thermal capacities denoted by C_g in Fig. 1c correspond to the region between the pipes and the borehole wall (V_{g1} and V_{g2} in Fig. 1b) while the thermal capacity C_{gg} corresponds to the central zone between the pipes (V_{gg}) as described by Pasquier and Marcotte (2012). The proposed model provides an improvement compared to the model of Pasquier and Marcotte as it accounts for the fluid circulation in the U-tube. In fact, the fluid temperature is calculated in each layer using energy balances. The heat transfer outside the borehole is assumed to be one-dimensional in the radial direction and is determined by using the infinite line source analytical solution applied to each axial layer.

2.1 Calculation of thermal resistances and thermal capacities

The thermal resistance R_{fp} defined in Eq. (1) includes the fluid convection resistance, R_f, and the pipe conduction resistance, R_p :

$$R_{fp} = R_f + R_p \tag{1}$$

The fluid convection resistance depends on the Nusselt number, *Nu*:

$$R_f = \frac{1}{Nu\, k_f\, \pi} \tag{2}$$

The pipe conduction resistance is the thermal resistance of a cylindrical wall given by:

$$R_p = \frac{\ln\left(\frac{r_o}{r_i}\right)}{2\,\pi\, k_p} \tag{3}$$

One of the challenges of this model is to accurately account for the two types of thermal interactions inside the borehole. The first interaction, between the pipes and the borehole wall, is characterized by the thermal resistances R_g. The second interaction, between the two pipes, is characterized by the thermal resistance R_{gg}. These two thermal resistances depend on the fluid-to-ground resistance, R_b, and the internal thermal resistance, R_a, which is also the total thermal resistance between the two pipes. These thermal resistances were originally introduced by the Delta-circuit of Eskilson and Claesson (1988), represented in Fig. 2a. The values for R_b and R_a are given by:

$$R_b = \frac{\frac{T_1 + T_2}{2} - \overline{T_b}}{q_1 + q_2} \tag{4}$$

$$R_a = \frac{2\,(T_1 - T_2)}{q_1 - q_2} \tag{5}$$

Where $\overline{T_b}$ is the mean temperature along the borehole circumference, and q_1, q_2 are the heat transfer rates exchanged by the two pipes. These values are obtained here using the multipole method (Bennet et al., 1987).

The thermal resistances R_g and R_{gg} are given by:

$$R_g = \frac{1}{2}\,(2\,R_b - R_{fp}) \tag{6}$$

$$R_{gg} = \frac{1}{2}\,\frac{4\,R_g\,(R_a - 2\,R_{fp})}{4\,R_g - (R_a - 2\,R_{fp})} \tag{7}$$

Each resistance of the Delta-circuit are divided into two sub-resistances (R_g and R_{gg}) in the proposed TRCM circuit which explains the factor $\frac{1}{2}$ in Eqs. (6) and (7).

For certain pipe spacings, Eqs. (4) and (5) can lead to negative values of R_{12}. Lamarche et al. (2010) explain that the use of a uniform temperature $\overline{T_b}$ on the borehole circumference causes these values to be negative. This assumption is inaccurate when the pipes are close to the borehole wall. Thus, they suggest to divide the borehole circumference into semicircles and define two temperatures $\overline{T_{b1}}$ and $\overline{T_{b2}}$ for each semicircle (Fig. 2b).

With this model, the thermal resistance R_{12} can be calculated using the following expression:

$$R_{12} = \frac{2\,(T_1 - T_2)}{q_1 - q_2 - \frac{T_1 - T_2 - (\overline{T_{b1}} - \overline{T_{b2}})}{R_1}} \tag{8}$$

This new thermal resistance R_{12} is then integrated into the Delta-circuit model to determine the internal thermal resistance R_a:

$$R_a = \frac{4\,R_{12}\,R_b}{4\,R_b + R_{12}} \tag{9}$$

R_{gg} is obtained using Eq. (7) with the internal thermal resistance R_a calculated with Eqs. (8) and (9). The two borehole temperatures, $\overline{T_{b1}}$ and $\overline{T_{b2}}$, are introduced to calculate the thermal resistance between the two pipes, R_{gg}. Thereafter, a single borehole temperature, $T_{b,i}$, is used for each axial layer.

The thermal capacities are given by:

$$C_g = V_g\, c_g = \frac{\pi\, {r_b}^2 - 4\, r_o\, D - \pi\, {r_o}^2}{2}\, c_g \tag{10}$$

$$C_{gg} = V_{gg}\, c_g = (4\, r_o\, D - \pi\, {r_o}^2)\, c_g \tag{11}$$

2.2 Governing equations

2.2.1 For each node of the proposed TRCM circuit

The following equations apply to the i^{th} layer of the borehole. At the pipe wall corresponding to node T_{g1} the governing equation is (A similar equation is used for node T_{g2}):

$$\frac{T_{1,i} - T_{g1,i}}{R_{fp}} + \frac{T_{g3,i} - T_{g1,i}}{R_g} + \frac{T_{g5,i} - T_{g1,i}}{R_{gg}} = 0 \tag{12}$$

In the grout, corresponding to node T_{g3} (A similar equation is used for node T_{g4}):

$$\frac{T_{g1,i} - T_{g3,i}}{R_g} + \frac{T_{b,i} - T_{g3,i}}{R_g} = C_g \frac{T_{g3,i} - T^0_{g3,i}}{\Delta t} \tag{13}$$

Finally, in the grouted central zone, corresponding to node T_{g5}:

$$\frac{T_{g1,i} - T_{g5,i}}{R_{gg}} + \frac{T_{g2,i} - T_{g5,i}}{R_{gg}} = C_{gg} \frac{T_{g5,i} - T^0_{g5,i}}{\Delta t} \tag{14}$$

In these equations, Δt is the simulation time step and the superscript "^{0}" refers to temperatures at the previous time step.

2.2.2 Energy balances

Energy balances for the downward and upward flowing fluid are calculated in each pipe sections. The two pipes of length L are divided into $2n_L$ sections, n_L sections for each of the downward and upward legs (Fig. 3). The derivation is based on the following assumptions: the mean fluid temperature ($T_{1,i}$ for the downward leg and $T_{2,i}$ for the upward legs) is assumed to be equal to the outlet temperature of the section being considered. For example, in the downward pipe, the fluid enters layer i with the outlet temperature of section i-1, i.e. $T_{1,i-1}$. The energy balance in the downward and upward directions for the i^{th} pipe section can be written as:

$$\frac{\dot{m}\, {c_p}_f}{L/n_L} \left(T_{1,i-1} - T_{1,i}\right) + \frac{T_{g1,i} - T_{1,i}}{R_{fp}} = \pi\, {r_i}^2 \rho_f\, {c_p}_f \frac{T_{1,i} - T^0_{1,i}}{\Delta t} \tag{15}$$

$$\frac{\dot{m}\, {c_p}_f}{L/n_L} \left(T_{2,i+1} - T_{2,i}\right) + \frac{T_{g2,i} - T_{2,i}}{R_{fp}} = \pi\, {r_i}^2\, \rho_f\, {c_p}_f \frac{T_{2,i} - T^0_{1,i}}{\Delta t} \tag{16}$$

with the boundary conditions:

$$T_{1,0} = T_{in} \tag{17}$$

$$T_{1,n_L} = T_{2,n_L+1} \tag{18}$$

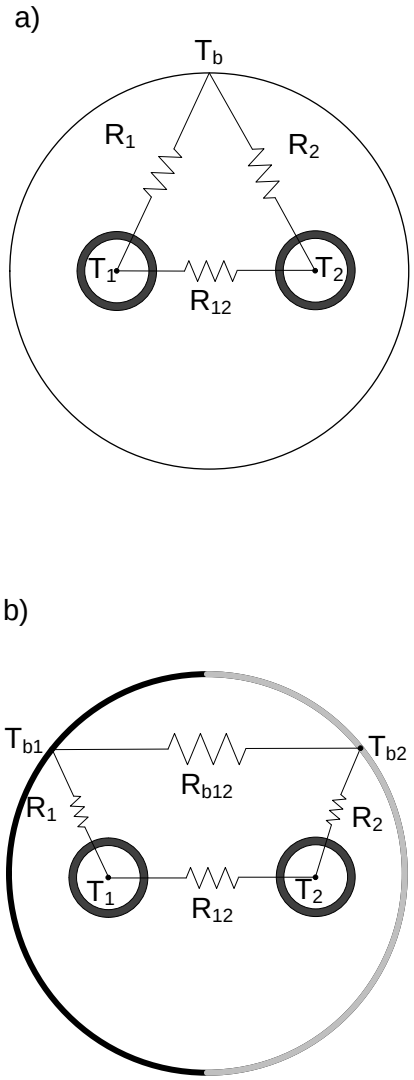


Figure 2: a) Original Delta-circuit (Eskilson & Claesson, 1988) and b) Thermal resistance model proposed by Lamarche et al. (2010)

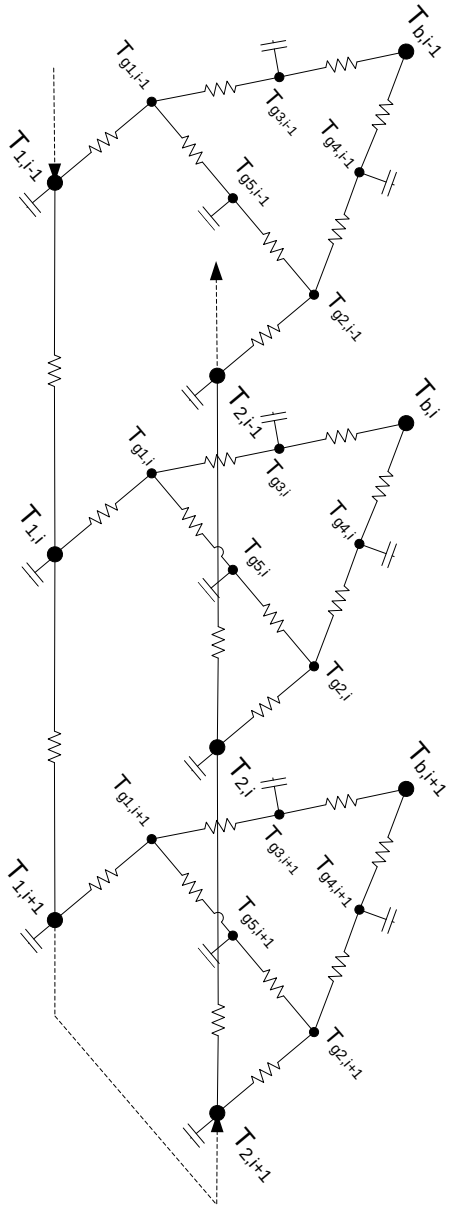


Figure 3: Schematic representation used to derived the energy balance in the vertical direction

2.2.3 Borehole wall

The borehole wall temperature is obtained using:

$$T_{b,i}(t) = T_0 + \Delta T_i(r_b, t) \quad (19)$$

T_0 is the undisturbed ground temperature and ΔT_i is the variation of the wall temperature of the i^{th} borehole layer and is defined as:

$$\Delta T_i(r_b, t) = Q_i \, h(r_b, t) \quad (20)$$

Where h is the ground response factor which is obtained using the infinite line source analytical solution to transient ground heat transfer.

Temporal superposition of Q_i is required due to a varying heat extraction rate. The aggregation method introduced by Liu (2005) is used to reduce the calculation time associated with temporal superposition.

The varying wall temperature of the i^{th} borehole layer at the end of the n^{th} time step is given by:

$$\Delta T_i(r_b, t = n\,\Delta t) = \sum_{j=1}^{n} q_i(t_j)\, h(t_n - t_j) \tag{21}$$

with

$$q_i(t_j) = Q_i(t_j) - Q_i(t_{j-1}) \tag{22}$$

Only the heat transfer rate of the last time step, $Q_i(t_n)$, is unknown and it is convenient to separate this term from the sum as suggested by Cimmino and Bernier (2013):

$$\Delta T_i(r_b, t = n\,\Delta t) = \Delta T_i^*(r_b, t = n\,\Delta t) + Q_i(t_n)\, h(t_n - t_{n-1}) \tag{23}$$

where :

$$\Delta T_i^*(r_b, t = n\,\Delta t) = \sum_{j=1}^{n-1} q_i(t_j)\, h(t_n - t_j) - Q_i(t_{n-1})\, h(t_n - t_{n-1}) \tag{24}$$

Finally, the wall temperature of i^{th} borehole layer is given by:

$$T_{b,i}(t = n\,\Delta t) = T_0 + \Delta T_i^*(r_b, t = n\,\Delta t) + Q_i(t_n) h(t_n - t_{n-1}) \tag{25}$$

2.2.4 Heat transfer rates

The heat transfer rate of the i^{th} borehole layer with the surrounding ground is:

$$Q_i = \frac{(T_{g3,i} - T_{b,i}) + (T_{g4,i} - T_{b,i})}{R_g} \tag{26}$$

2.3 Solution procedure

A total of 9 equations should be solved for each layer:

- 5 equations corresponding to each node of the TRCM circuit, i.e. Eqs. (12), (13), and (14),
- 2 energy balances, Eqs. (15) and (16),
- The borehole wall temperature, Eq. (25),
- The heat transfer rate, Eq. (26).

In addition to the $9n_L$ equations, two boundary conditions are required, i.e. Eqs. (17), and (18). Finally, the problem can be rewritten as a matrix system of $9n_L$+2 equations:

$$[A].\{X\} = \{B\} \tag{27}$$

Where *[A]* is the matrix of the coefficient, $\{X\}$ is the vector of unknowns and $\{B\}$ is the vector of known terms. Matrix [A] is inverted to determine the unknown stored in the vector $\{X\}$:

$$\{X\} = [A]^{-1}.\{B\} \tag{28}$$

The proposed TRCM model has been implemented as a component (TYPE) in the TRNSYS environment. This enables its use with other models (building, heat pumps, etc.) in annual energy simulations.

3 INTER-MODEL COMPARAISON

The proposed TRCM model is compared to three existing models that account for transient behavior in borehole heat exchangers: the “General Elliptical Multi-Block Solver” (GEMS2D and GEMS3D) of He (2012) and the EWS model of Wetter and Huber (1997) known as “TYPE 451” in TRNSYS.

GEMS2D solves numerically the two-dimensional advection-diffusion equation while GEMS3D solves the three-dimensional equation, and simulates fluid transport inside the U-tube and axial heat transfer in and around the borehole heat exchanger.

The EWS model (Wetter & Huber, 1997) uses the concept of capacitance/resistance. It is a 2D model which accounts for fluid and grout thermal capacities in double U-tube borehole heat exchangers which is transformed into an equivalent single pipe. In the radial direction, the borehole and the surrounding ground are divided into non-uniform grids. Heat transfer is evaluated by solving numerically the one-dimensional heat equation while the outer boundary condition is calculated by the infinite line source analytical solution. Only one node is used to account for the entire grout thermal capacity. In the axial direction, the borehole is subdivided into several equidistant layers. The fluid temperature is calculated in each layer using transient energy balances. In the present case, the EWS model has been modified and adapted to a single U-tube geometry to make a fair comparison between the proposed TRCM and the EWS models.

The following comparison is based on the work of He et al. (2009). In this comparison a borehole is subjected to sudden inlet temperature changes from 10°C to 20°C every 15 minutes. The borehole parameters and ground thermal properties are shown in Table 1. The results are presented in Fig. 4 where the outlet temperatures obtained with the proposed TRCM model, the EWS model and the GEMS2D/GEMS3D models are compared.

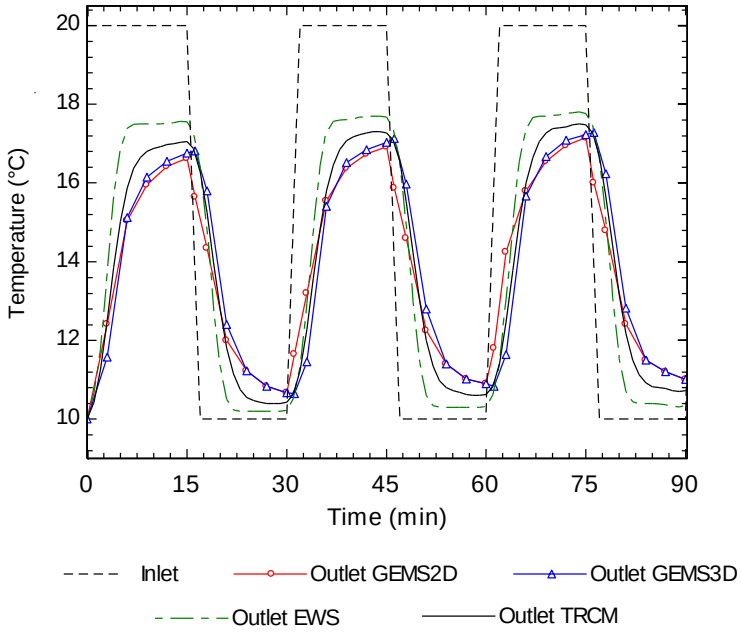


Figure 4: Comparison of the proposed TRCM model against the EWS (Wetter & Huber, 1997) and the He et al. (2009) models

Table 1: Parameters used for the validation

Parameter	Unit	Value
Borehole		
L	m	100
r_b	m	0.075
r_i	m	0.0131
r_o	m	0.016
D	m	0.0322
k_f	$W.m^{-1}.K^{-1}$	0.6
$(\rho c_p)_f$	$MJ.m^{-3}.K^{-1}$	4.2
k_p	$W.m^{-1}.K^{-1}$	0.39
$(\rho c_p)_p$	$MJ.m^{-3}.K^{-1}$	1.77
k_{gt}	$W.m^{-1}.K^{-1}$	0.75
$(\rho c_p)_{gt}$	$MJ.m^{-3}.K^{-1}$	3.9
Ground		
T_g	°C	10
k_{gr}	$W.m^{-1}.K^{-1}$	2.5
$(\rho c_p)_{gr}$	$MJ.m^{-3}.K^{-1}$	2.5
Fluid velocity		
v	$m.s^{-1}$	1

The GEMS3D results are used here as the reference. Results show that the TRCM model follows the trend observed for the GEMS3D for the outlet temperature. The TRCM results are in better agreement than the EWS results when compared to the GEMS3D results. The RMS difference between the TRCM and the GEMS3D results is 0.59°C while the corresponding difference between the EWS and the GEMS3D results is 1.2°C. Fully discretized 3D models such as the GEMS3D are highly desirable for their accuracy. However, they are not yet suitable for implementation in energy simulation software tools that perform annual simulations. In that context, the proposed TRCM model appears to be a good compromise between calculation time and results accuracy. Moreover, the proposed TRCM is easily implementable in most energy simulation software tools.

It is to be noted that the TRCM model was also run with the cylindrical heat source analytical solution for ground heat transfer for the test case presented in Fig.4. Results were essentially the same as those obtained with the infinite line source.

4 EFFECTS OF FLUID AND GROUT THERMAL CAPACITIES

The effects of the fluid and grout thermal capacities on the heat pump energy consumption will now be examined with a case study using the proposed TRCM model in the TRNSYS environment.

The case study concerns a ground-source heat pump system used to heat and cool a well-insulated house in a cold climate (Montreal, Canada). The main building characteristics are given in Table 2a. The building is equipped with a 1.5 ton capacity (5.3 kW) heat pump with two electric auxiliary heaters (5 kW each). In heating mode, the heat pump starts when the temperature is less than 21°C. The first and second stage auxiliary heaters are energized when the temperature reaches 20°C and 19°C, respectively. The cooling mode set point is 25°C. Annual simulations with this control scenario indicate that the annual heating and cooling needs are 9.5 MWh and 6 MWh, respectively. The heat pump is linked to a borehole ground heat exchanger whose characteristics are given in Table 2b.

Four cases are considered in the following sections to illustrate thermal capacity effects. In the first case, both the fluid and grout thermal capacities (WFG, acronym for **W**ith **F**luid and **G**rout capacities) are accounted for. In the second case, only the fluid thermal capacity (WF-WOG) is considered while only grout thermal capacity (WOF-WG) is accounted in the third case. Finally in the last case, both thermal capacities (WOFG) are neglected.

4.1 On/off cycles

For this first set of results, the heat pump is controlled manually and on/off cycles of 8 h, 2 h, 30 min and 10 min are applied. In this case, the circulating pump is always on.The predicted borehole outlet temperature is calculated with a 5 min time step and shown in Fig. 5 for the four cases previously identified. The two cycles of 8 h and 2 h represent cases where the heat pump operates for a relatively long time approaching a quasi-steady-state condition while the two other cycles of 30 min and 10 min are more representative of intermittent on-and-off operation.

At the beginning of each pulse, the predicted outlet temperature of cases considering at least one thermal capacity (WFG, WF-WOG, and WOF-WG) change gradually with the WFG case having the most gradual change. However, the predicted outlet temperature of the WOFG case decreases abruptly. After one time step, the outlet fluid temperature from the WOFG and WFG cases differ by about 2.5°C. This difference would lead to differences in the

evaluation of the heat pump energy consumption. After this initial transient period, the outlet temperatures predicted by the four cases tend towards the same values.

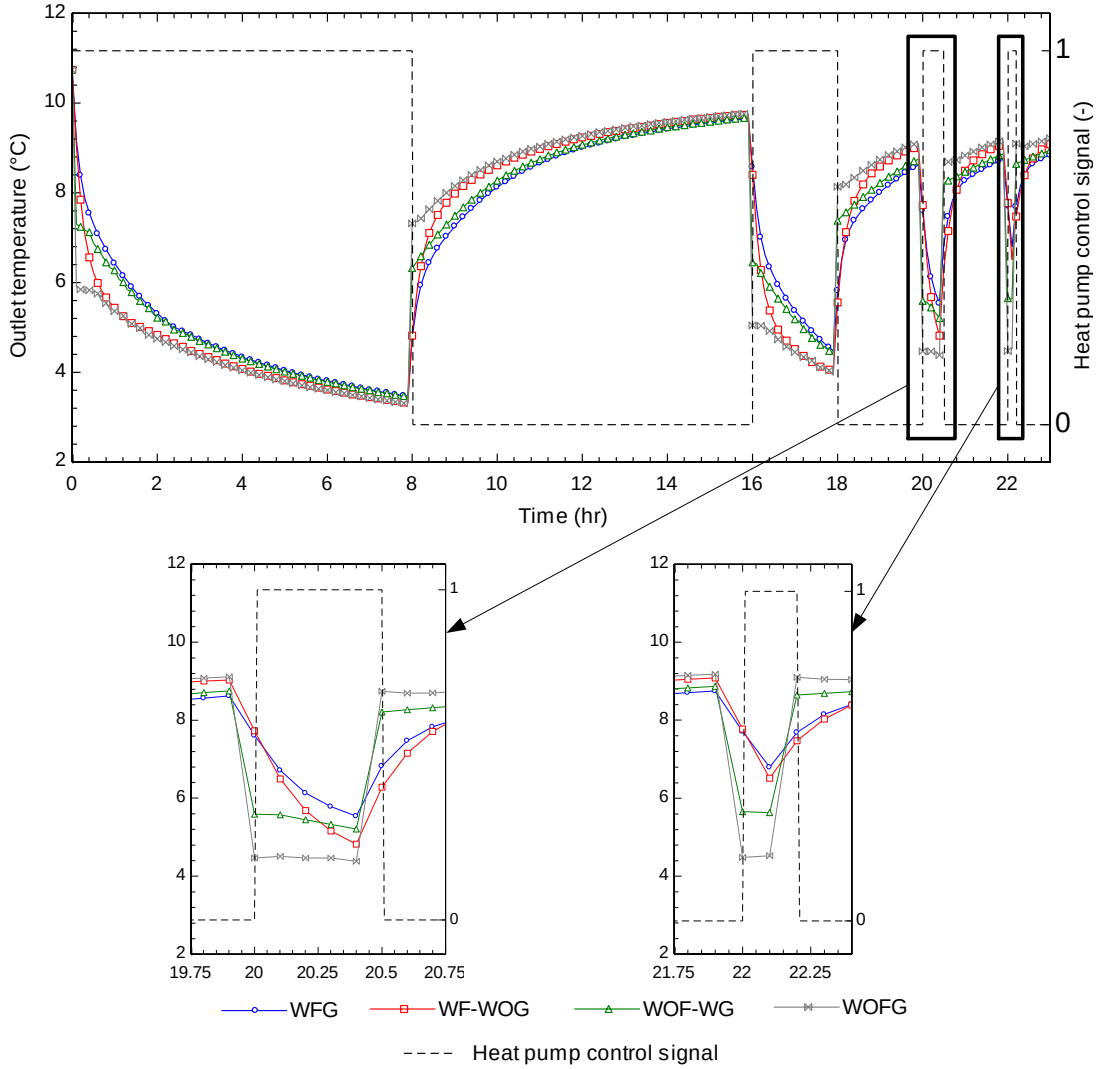


Figure 5: Fluid temperature variations during hourly pulses

For the short cycles (30 min and 10 min), the WF-WOG and WFG case are in closer agreement. For the 10 min cycle, the maximum difference between the WF-WOG and WFG cases is 0.28°C while the corresponding difference between the WOF-WG and WFG is 2.06°C. This seems to indicate that the fluid thermal capacity is the dominant factor when boreholes transients are accounted for and that grout capacity plays a minor role.

4.2 Annual simulations

The effect of the borehole thermal capacity on the annual energy consumption of a heat pump will now be examined using the proposed TRCM model in TRNSYS (v17). The simulations are performed for three different commercially available heat pumps, each with a 1.5 ton nominal capacity but with different COPs as shown in Fig. 6. These heat pumps were selected to examine the impact of heat pumps that react differently with a change of the entering water temperature (EWT). For example, HP 1 has a COP variation with EWT (i.e. slope) which is higher than the other two.

In addition, the simulations are performed for 4 different borehole depths (60-80-120-160m). The 60 m and 160 m depths represent boreholes that are undersized and oversized,

respectively. Each annual simulation is run with the four thermal capacity scenarios identified earlier. A total of 48 annual simulations are thus carried out with a 3 min simulation time step. The results of these simulations are shown in Fig.7 where the heat pump energy consumptions, Q_{el}, and the annual average COPs are plotted as a function of borehole depth.

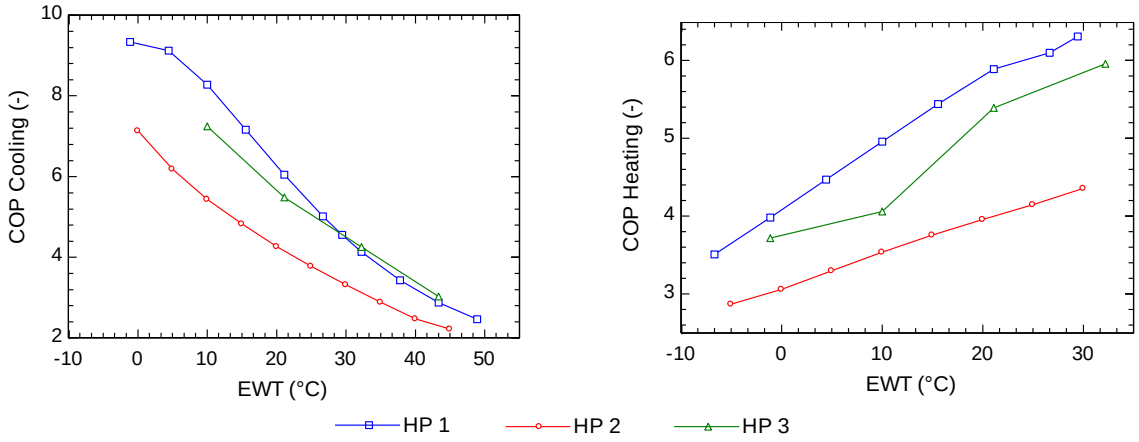


Figure 6: COP as a function of the entering water temperature for 3 different heat pumps

Table 2: a) Building characteristics, b) ground and borehole thermal properties and c) total fluid and grout thermal capacity for a 120 m borehole

a)

Parameter	Unit	Value
Building characteristics		
Heated aera	m²	220
Conditioned volume	m^3	525
Windows aera	m²	20.6
Thermal performance		
R external walls	$m^2.K.W^{-1}$	6
R ceiling	$m^2.K.W^{-1}$	7.7
R basement walls	$m^2.K.W^{-1}$	4.3
R floor	$m^2.K.W^{-1}$	1.6
Windows *U*-value	$W.m^{-2}.K^{-1}$	1.4

b)

Parameter	Unit	Value
Borehole		
L	m	60 – 80 - 120 -160
r_b	m	0.075
r_i	m	0.013
r_o	m	0.016
D	m	0.059
k_p	$W.m^{-1}.K^{-1}$	0.39
Fluid (propylene glycol 30%)		
k_f (10°C)	$W.m^{-1}.K^{-1}$	0.44
$(\rho c_p)_f$ (10°C)	$MJ.m^{-3}.K^{-1}$	4.0
Grout		
k_{gt}	$W.m^{-1}.K^{-1}$	0.75
$(\rho c_p)_{gt}$	$MJ.m^{-3}.K^{-1}$	3.9
Ground		
k_{gr}	$W.m^{-1}.K^{-1}$	2
$(\rho c_p)_{gr}$	$MJ.m^{-3}.K^{-1}$	2.3

c)

Parameter	Unit	Value
Total thermal capacity (*L*=120 m)		
Fluid	$MJ.\ K^{-1}$	0.5
Grout	$MJ.\ K^{-1}$	7.7

It is possible to observe the same trend in all 48 simulations. First, the heat pump energy consumption prediction is lower for deeper boreholes. This was to be expected as deeper boreholes lead to more favorable entering water temperature to the heat pump. Second, the heat pump energy consumption prediction is higher when the borehole thermal capacity is ignored.

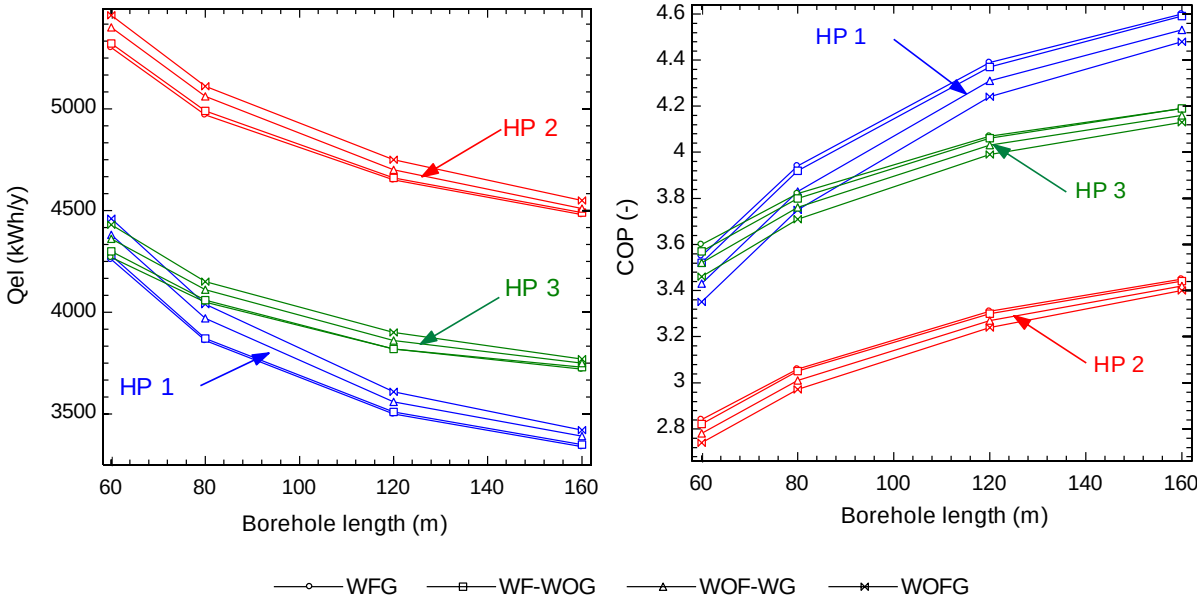


Figure 7: Yearly energy performance comparison

This over prediction is higher when the variation of the COP with EWT is high (such as for HP1) and the borehole is undersized. The annual energy consumption differences between these cases are shown in Table 3. In this table, the results for all borehole depths have been averaged. Results for HP1 will be examined; conclusions for HP2 and HP3 are similar. These results show that on annual basis, the energy consumption (on average for all borehole depths) is 3.6% lower when the grout and fluid thermal capacities (WFG) are accounted for. These results corroborate the results of Salim-Shirazi and Bernier (2013). It is interesting to note that if the fluid capacity is accounted for but the grout thermal capacity is not considered (WF-WOG), the difference decreases by a small amount from 3.6% down to 3.3%. When only the grout capacity is considered (WOF-WG) the difference is reduced to 1.4%. This seems to indicate that the fluid thermal capacity has a greater effect than grout thermal capacity.

The over prediction is also higher when the boreholes are undersized. For example, the difference in annual energy consumption reaches 4.7% for HP 1 and for a 60m borehole (not shown in Table 3). This difference is explained by the ground temperature which is more affected because of the undersized borehole.

Table 3: Energy consumption differences (in %) with respect to the WOFG case (average for all borehole lengths)

Heat pump	WFG	WF-WOG	WOF-WG
HP 1	3.6%	3.3%	1.4%
HP 2	2.3%	2.0%	1.0%
HP 3	2.3%	2.1%	1.0%

5 CONCLUSION

A borehole heat exchanger model, based on the TRCM concept, has been developed and presented in this paper. The proposed model integrates the grout and the fluid thermal capacity of the borehole and considers the fluid transport inside the U-tube. The proposed TRCM model has been implemented as a component (TYPE) in the TRNSYS environment. It

was compared with other models, and showed good agreement including against a fully discretized 3D model. Then, the proposed model was used in simulations of a ground-source heat pump system. Results from these simulations show that neglecting fluid and grout thermal capacities leads to an overestimation of the annual heat pump energy consumption by ≈ 3%. The overestimation is greater with undersized boreholes and with heat pump that have a high COP variation with the entering water temperature. Finally, results shown here seem to indicate that the fluid capacity has a greater impact than grout capacity.

6 REFERENCES

Bauer, D., Heidemann, W., Müller-Steinhagen, H., & Diersch, H.-J. (2011). Thermal Resistance and Capacity Models for Borehole Heat Exchangers. *International Journal of Energy Research, 35*(4), 312-320.

Bennet, J., Claesson, J., & Hellstrom, G. (1987). *Multipole Method to Compute the Conductive Heat Flows to and Between Pipes in a Composite Cylinder*. Lund, Sweden.

Cimmino, M., & Bernier, M. (2013). *Preprocessor for the Generation of the G-Functions Used in the Simulation of Geothermal Systems*. Paper presented at the 13th Conference of International Building Performance Simulation Association, Chambéry, France.

Eskilson, P., & Claesson, J. (1988). Simulation Model for Thermally Interacting Heat Extraction Boreholes. *Numerical Heat Transfer, 13*(2), 149-165.

He, M. (2012). *Numerical Modelling of Geothermal Borehole Heat Exchanger Systems.* Ph.D., Montfort Universoty, Leicester, UK.

He, M., Rees, S. J., & Shao, L. (2009). *Applications of a Dynamic Three-Dimensional Numerical Model for Borehole Heat Exchangers*. Paper presented at the the 11th International Conference on Thermal Energy Storage, Stockholm Internal Fairs, Stockholm, Sweden.

Hellstrom, G. (1991). *Ground Heat Storage: Thermal Analysis of Duct Storage Systems: Part 1 Theory.* PhD, University of Lund, Lund.

Kummert, M., & Bernier, M. (2008). Sub-hourly simulation of residential ground coupled heat pump systems. *Building Service Engineering Research and Technology, 29*(1), 27-44.

Lamarche, L., Kajl, S., & Beauchamp, B. (2010). A Review of Methods to Evaluate Borehole Thermal Resistances in Geothermal Heat-Pump Systems. *Geothermics, 39*(2), 187-200.

Pasquier, P., & Marcotte, D. (2012). Short-Term Simulation of Ground Heat Exchanger with an Improved TRCM. *Renewable Energy, 46*, 92-99.

Salim-Shirazi, A., & Bernier, M. (2013). Thermal Capacity Effects in Borehole Ground Heat Exchangers. *Energy and Buildings, 67*, 352-364.

Wetter, M., & Huber, A. (1997). TRNSYS Type 451: Vertical Borehole Heat Exchanger EWS Model, Version 3.1 - Model description and implementing into TRNSYS. In T. GmbH (Ed.). Stuttgart, Germany.

Zarella, A., Scarpa, M., & De Carli, M. (2011). Short Time Step Analysis of Vertical Ground-Coupled Heat Exchangers: The Approach of CaRM. *Renewable Energy, 36*(9), 2357-2367.